Biomedicine & Pharmacotherapy 189 (2025) 118246

Contents lists available at ScienceDirect

Biomedicine & Pharmacotherapy

journal homepage: www.elsevier.com/locate/biopha

Identification of nsp16 inhibitors of SARS -CoV-2, SARS -CoV-1 and MERS-CoV from FDA-approved drugs using *in silico* and *in vitro* methods

Ejlal A. Omer [a], Sara Abdelfatah [a], Nasim Shahhamzehei [a], Axel Guthart [a], Kathrin Sutter [b,c], Hannah S. Schwarzer-Sperber [b], Roland Schwarzer [c,*], Thomas Efferth [a,*]

[a] Department of Pharmaceutical Biology, Institute of Pharmaceutical and Biomedical Sciences, Johannes Gutenberg University, Staudinger Weg 5, Mainz 55128, Germany
[b] Institute for Virology, University Hospital Essen, University Duisburg-Essen, Essen, Germany
[c] Institute for the Research on HIV and AIDS-associated Diseases (HIV-AAD), University Hospital Essen, University Duisburg-Essen, Essen, Germany

ARTICLE INFO

Keywords:
Pan-coronavirus inhibitors
Nsp16
FDA-approved drugs
SARS-CoV-2

ABSTRACT

The methyltransferase nsp16 is a key enzyme that catalyses coronavirus replication. In this study, we virtually screened 1577 FDA-approved drugs against nsp16 of SARS-CoV-2, SARS-CoV-1, and MERS-CoV to identify compounds potentially serving as pan-coronavirus inhibitors. Microscale thermophoresis (MST) was used to verify the *in-silico* results obtained by virtual drug screening, followed by molecular docking and molecular dynamics simulation to test the binding affinities between the target and the candidates. Finally, the candidates were tested against a clinical isolate of SARS-CoV-2 in cell culture. The MST binding assay and molecular docking results showed that four of the candidates showed strong binding affinities to nsp16 of one or two coronaviruses. Nilotinib and simeprevir interacted with nsp16 protein of all three coronaviruses, *viz.*, SARS-CoV-2, SARS-CoV-1, and MERS-CoV, suggesting their potential to act as pan-coronavirus inhibitors. The drugs inhibited the virus with IC_{50} values ranging between 8.34 and 36.1 μM when tested against a clinical isolate of SARS-CoV-2 in cell culture.

1. Introduction

RNA viruses are phenotypically and genetically highly diverse, and their hosts include both vertebrates and invertebrates. Therefore, they have a powerful impact on human public health, as well as livestock and agriculture. Due to the zoonotic origin and mutative ability of RNA viruses, new species and variants continuously emerge from animal reservoirs that are potentially pathogenic to humans [1,2]. As a result, RNA viruses represent a critical challenge for global disease control, which was recently highlighted by the SARS-CoV-2 pandemic [3]. SARS-CoV-2 infected more than 778 million people and caused more than 7 million fatalities worldwide [4]. The SARS-CoV-2 genome underwent rapid mutation since its first appearance in 2019 and still continuously evolves. Consequently, several variants came up which are known as variants of concern (VOCs). These variants include Alpha, Beta, Gamma, Delta, and Omicron variants [5].

SARS-CoV-2 is classified alongside the previously emerged SARS-CoV-1 and MERS-CoV, all of which belong to the *Coronaviridae* family under the order *Nidovirales*. They have a large RNA genome, consisting of about 30,000 nucleotides, which contains structural and non-structural proteins, as well as accessory proteins [6,7]. Non-structural proteins include viral proteases, RNA-dependent RNA polymerase, and methyltransferases, which are indispensable for virus replication, translation, and proliferation [8–10].

The coronavirus mRNA is capped at its 5′ end, which is crucial for virus replication. The cap installation process is completed with a methylation step, catalyzed by non-structural protein 16 (nsp16), utilizing S-adenosyl-L-methionine (SAM) as a substrate. Nsp16 methyltransferase is a highly conserved protein among coronaviruses [11,12]. Moreover, it has a mutational frequency of less than 0.04 %, being identical in 90.74 % of all samples tested worldwide. As a result, it is considered a potential drug target due to its resistance to viral evolution in the future [5]. It has been reported that the disruption of nsp16 binding to its substrate SAM, inhibits the protein's activity and consequently virus replication [13,14]. Notably, the coronavirus cap contains C2′-O-methylrybosyladenine and N-methylated guanosine triphosphate, which are highly homologous to their eukaryotic counterparts. These structural similarities between the virus and its host protect the virus

* Corresponding authors.
E-mail addresses: Roland.Schwarzer@uk-essen.de (R. Schwarzer), efferth@uni-mainz.de (T. Efferth).

https://doi.org/10.1016/j.biopha.2025.118246
Received 15 April 2025; Received in revised form 23 May 2025; Accepted 10 June 2025
Available online 20 June 2025

Table 1
Virtual drug screening of selected candidates and the natural substrate SAM (control compound) for binding to nsp16 of SARS-CoV-2, SARS-CoV-1, and MERS-CoV. PyRx has been used for screening against all the nsp16 proteins and MOE for docking to the nsp16 of SARS-CoV-2.

Ligand	Lowest binding energy (kcal/mol) of ligands bound to nsp16 using PyRx			S-scores of ligands bound to nsp16 using MOE
	SARS-CoV-2	SARS-CoV-1	MERS-CoV	SARS-CoV-2
Eltrombopag	–11.0	–8.1	–7.6	–7.42 ± 0.64
Ponatinib	–10.8	–7.7	–7.5	–8.01 ± 0.75
Teniposide	–10.7	–7.7	–8.4	–9.09 ± 0.61
Conivaptan	–10.6	–7.7	–7.6	–8.00 ± 0.61
Lifitegrast	–10.6	–8.2	–8.7	–8.49 ± 0.29
Simeprevir	–10.6	–6.6	–7.9	–9.02 ± 0.45
Imatinib	–10.4	–8.1	–7.5	–7.98 ± 0.69
Ecamsule	–10.4	–7.6	–7.5	–7.70 ± 0.16
Dihydroergotamine	–10.3	–7.9	–8.3	–7.94 ± 0.64
Nilotinib	–10.2	–8.5	–8.0	–8.08 ± 0.31
SAM	–7.70	–7.10	–6.30	–7.43 ± 0.45

from being recognized by the host's immune system, allowing the virus to use the host's translational machinery [15–17]. However, there is a distinct difference in the cap installation process between humans and viruses, making virus enzymes an attractive target for antiviral drugs. Therefore, targeting nsp16 in coronaviruses serves as a promising target for novel pan-coronaviral inhibition [18].

The concept of drug repurposing is a well-known strategy [19,20]. In fact, 30–40 % of drugs approved by the Food and Drug Administration (FDA) between 2007 and 2009 were repurposed drugs [21–23]. Using an FDA-approved drug library opens the possibility to accelerate drug development, and reduce costs, since a substantial amount of pharmacokinetic and toxicological data has already been gathered for approved drugs. Compared with *de novo* drug development, drug repurposing has higher success rates of drug candidate identification (30 % *vs.* 10 % for *de novo* drugs), as well as the rapid clinical use of drugs (3–12 years

Table 2
K_d values of the candidates bound to nsp16 of SARS-CoV-2, SARS-CoV-1, and MERS-CoV as measured by microscale thermophoresis. The results are shown as mean values ± SD of at least two independent experiments.

Candidate	K_d values (μM) of candidates bound to nsp16 proteins		
	SARS-CoV-2	SARS-CoV-1	MERS-CoV
Nilotinib	1.68 ± 0.44	5.21 ± 1.10	29.86 ± 2.96
Lifitegrast	24.01 ± 0.18	-	-
Dihydroergotamine	28.56 ± 5.51	-	94.2 ± 3.13
Eltrombopag	48.74 ± 1.04	-	-
Simeprevir	71.18 ± 2.26	90.10 ± 4.44	88.85 ± 0.92

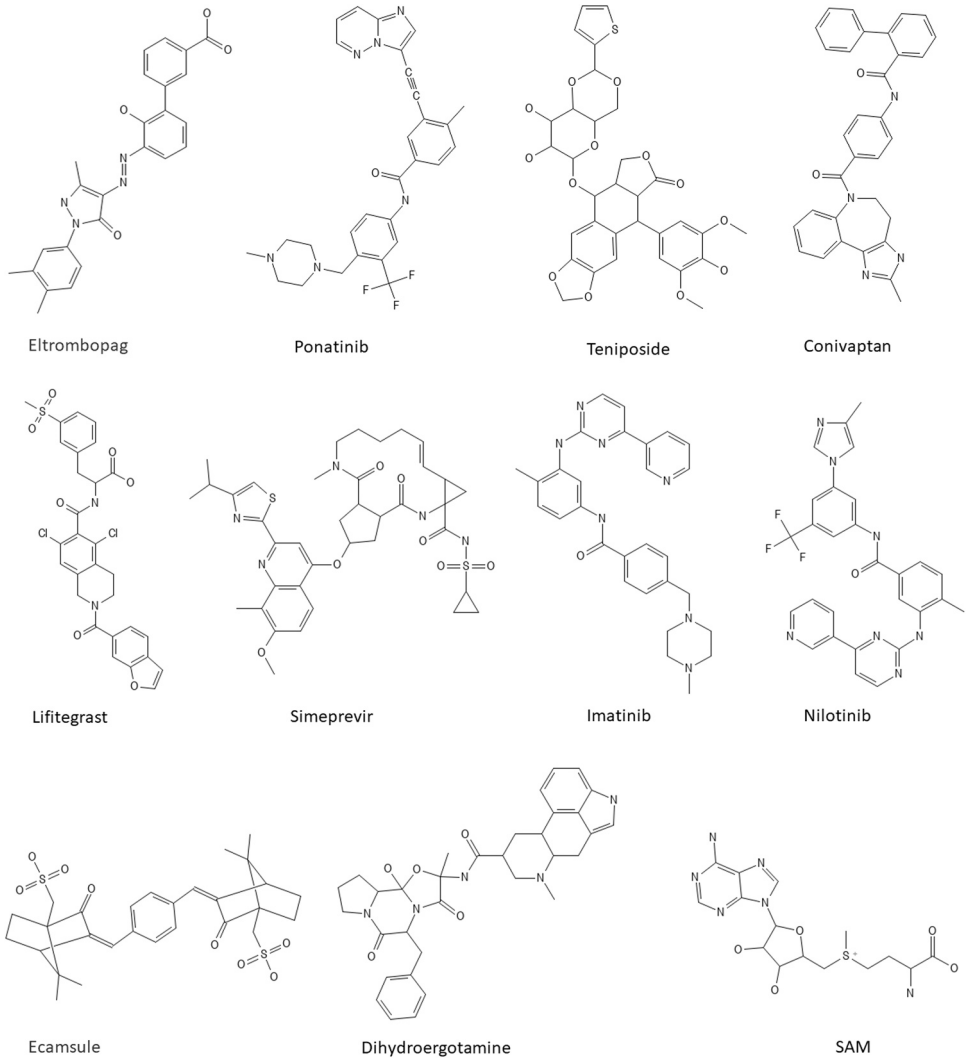

Fig. 1. Chemical structures of the selected ligands. PubChem Sketcher V2.4 was used for drawing the structures.

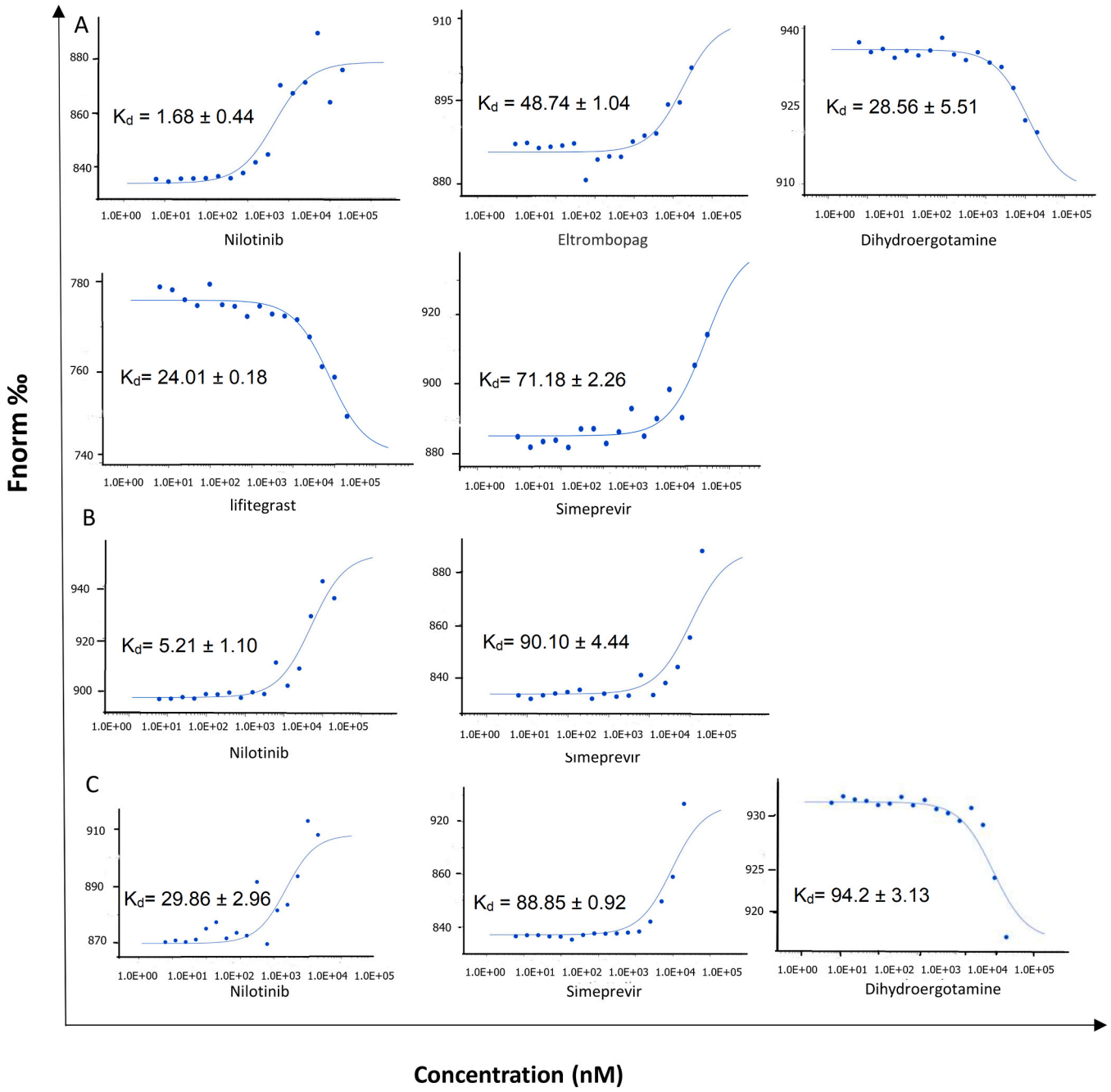

Fig. 2. Binding of the drug candidates to nsp16 of SARS-CoV-2 (A), SARS-CoV-1 (B), and MERS-CoV (C) as measured by microscale thermophoresis.

compared with 10–17 years for *de novo* drugs). An additional advantage is the improved economic affordability due to substantially reduced costs during the drug development process [23]. Consequently, drug repurposing has been suggested as an attractive choice for drug discovery, especially in pandemic crises.

Although we aimed to identify pan-coronavirus inhibitors targeting nsp16 in a previous study [18], the concept of the present study is different. While in our previous investigation we screened candidates from a natural product-based library of 224,205 compounds obtained from the ZINC database, in the present investigation we focused on 1577 FDA-approved drugs. The chemical library of 224,205 natural product-based compounds was previously used to identify novel candidate compounds that may serve for further drug development. Therefore, highlighting the methodological difference between the present study and our previous one. In the present study, we verified drug screening and molecular docking findings by molecular dynamics simulations which gave us deeper insights into candidate-protein binding properties than molecular docking alone. The binding of the candidate compounds to nsp16 was further characterized by microscale thermophoresis in vitro. To verify the antiviral activity of the compounds identified in silico, we also tested the candidates using clinical isolates of SARS-CoV-2 and a cellular infection assay.

2. Materials and methods

2.1. Virtual screening of ligands

The PyRx software was used for virtual screening of 1577 FDA-approved drugs to study their binding to the nsp16 protein of SARS-CoV-2. The 1.8 Å crystal structure of the nsp16-nsp10 complex of

Table 3
Molecular docking of the top candidate compounds and the natural substrate SAM to nsp16 of SARS-CoV-2, SARS-CoV-2, and MERS-CoV. The results are shown as mean values ± SD of three independent runs.

Nsp16	Ligand	S-scores using MOE
SARS-CoV−2 (PDB: 6W4H)	Nilotinib	–8.08 ± 0.31
	Lifitegrast	–8.49 ± 0.29
	Dihydroergotamine	–7.94 ± 0.64
	Eltrombopag	–7.42 ± 0.64
	Simeprevir	–9.02 ± 0.45
	SAM	–7.43 ± 0.04
SARS-CoV−1 (PDB: 3R24)	Nilotinib	–8.67 ± 0.15
	Simeprevir	–10.09 ± 0.47
	SAM	–7.87 ± 0.29
MERS-CoV (PDB: 5YN6)	Nilotinib	–8.77 ± 0.45
	Dihydroergotamine	–8.86 ± 0.30
	Simeprevir	–10.14 ± 0.79
	SAM	–9.14 ± 1.12

SARS-CoV-2 (PDB: 6W4H), used for virtual drug screening, was downloaded from the Protein Data Bank (www.rcsb.org). The top 100 ligands obtained with a cut-off value of –9.1 kcal/mol were rescreened against nsp16 of both SARS-CoV-1 and MERS-CoV (PDB: 3R24 and 5YN6, respectively).

2.2. Compounds and recombinant proteins

The selected ligands were purchased from MedChemExpress Europe (Sollentuna, Sweden). Recombinant nsp16 proteins of SARS-CoV-2, SARS-CoV-1, and MERS-CoV were purchased from the Medical Sciences Institute, School of Life Sciences, The University of Dundee (Dundee, Scotland). The product codes were GST-NSP16 SARS-CoV-2 (DU66420), GST-NSP16 SARS-CoV-1 (DU75116), and GST-NSP16 MERS-CoV (DU75117).

2.3. Microscale thermophoresis

Microscale thermophoresis (MST) was used to confirm the interaction between selected ligands and nsp16 *in vitro* as previously described [18]. The nsp16 proteins of SARS-CoV-2, SARS-CoV-1, and MERS-CoV were labelled using the Monolith™ NT.115 Protein Labelling Kit BLUE-NHS (NanoTemper Technologies GmbH, Munich, Germany). Nanodrop 1000 (Thermo Fisher Scientific, Wilmington, USA) was used to measure the concentration of the labelled protein. Sixteen serial dilutions ranging from 300 μM to 0.0091 μM of each ligand were prepared in the assay buffer (50 mM Tris buffer, pH 7.6, containing 150 mM NaCl, 10 mM $MgCl_2$, and 0.05 % Tween-20). The labelled protein was mixed with ligands (1:1) and incubated for 30 min at room temperature. The final concentration of the proteins was 133 nM, 99.5 nM, and 192.7 nM for nsp16 of SARS-CoV-2, SARS-CoV-1, and MERS-CoV, respectively. After incubation, the 16 samples were loaded into the capillaries in the NanoTemper Monolith™ NT (NanoTemper Technologies GmbH, Munich, Germany). The light emitting diodes (LED) power was set to 50 %, and the laser power was adjusted to 20 %, 40 %, and 60 %. The software MO. Affinity Analysis was used to analyze the data, generate the fit curves, and calculate the dissociation constants (K_d). K_d was calculated using a concentration-dependent measurement of the diffusion constant D.

Ligands that showed *in vitro* binding to nsp16 of SARS-CoV-2 were reinvestigated for their binding ability to nsp16 of SARS-CoV-1 and MERS-CoV. The K_d values were the average obtained from a minimum of two independent experiments for each tested protein.

2.4. Molecular docking of hits to coronaviral nsp16 binding pocket

Using Molecular Operating Environment (MOE, 2022.02, Chemical Computing Group, Montreal, Canada), ligands that showed binding in MST were docked to nsp16 proteins of SARS-CoV-2, SARS-CoV-1, and MERS-CoV (PDB: 6W4H, 3R24, and 5YN6, respectively). The known nsp16 substrate S-adenosyl methionine (SAM) served as a positive control substance. The proteins were prepared by the software, hydrogens were added, missing residues were repaired, and the protonation states were assigned. The energy of the protein and each of the ligands was minimized. The molecules were docked to the binding pocket. The induced fit model was selected, in which 100 poses were created and 50 refinements for each ligand. Three independent runs were performed for each of the candidates against the three targeted proteins. The scoring energy values were predicted by utilizing the London dG scoring function. The receptor-ligand binding affinities for all potential binding geometries were ranked according to a numerical metric referred to as the S-score, the lowest S-scores indicating the highest binding affinity. 2D interactions of amino acids with ligands were shown using MOE, whereas the 3D representations were generated using BIOVIA Discovery Studio Visualizer (https://discover.3ds.com/discovery-studio-visualizer-download). The images were created by Discovery Studio Visualizer V 21.1.0.20298 (Dassault Systemes Biovia Corp, USA).

2.5. SARS-CoV-2 propagation and quantification

A SARS-CoV-2 isolate (assigned to B.1.1.10 according to Pangolin database accession number EPI_ISL_602518) derived from patient material was used for infection experiments as previously described [24]. The virus was produced in Vero E6 cells, plated at a concentration of 2×10^6 Vero E6 cells in a T75 flask, and incubated for 24 h at 37 °C with 5 % CO_2 in Dulbecco's modified Eagle's medium (DMEM) supplemented with 10 % fetal bovine serum (FBS), 1 % L-glutamine, 1 % penicillin, and 1 % streptomycin. Subsequently, cells were exposed to the isolated virus and incubated for an additional 72 h. Afterwards, the culture supernatant was clarified by centrifugation and stored at –80 °C. Viral concentrations were assessed using an endpoint dilution assay to determine the 50 % tissue culture infective dose ($TCID_{50}$).

2.6. SARS-CoV-2 In-Cell ELISA procedure

Virus infection was quantified by In-Cell ELISA following a recently published protocol [25]. A total of 2×10^4 cells were seeded per well in a flat-bottom 96-well plate one day prior to infection. Then, the medium was aspirated, and serially diluted compounds and SARS-CoV-2 with a final concentration of 350 PFU/mL were added to cells for 24 h and subsequently fixed using 4 % paraformaldehyde in PBS. Permeabilization was conducted using a 1 % Triton-X-100 solution in PBS, followed by blocking with 3 % FCS in PBS. Next, the primary antibody (anti-N mAb1 ABIN6952435, Antibodies Online, Aachen, Germany) was added and incubated for 2 h at room temperature. Subsequently, a peroxidase-labeled secondary antibody (Cat. # 115-035-003, Jackson Immuno Research, Cambridge, UK) was applied for an additional hour, followed by washing steps with a solution of 0.05 % Tween-20 in PBS. Finally, the tetramethylbenzidine (TMB) substrate was added, and the enzymatic reaction was terminated using 0.5 M HCl. The absorbance of the dye was then measured at 450 nm using a Spark® 10 M multimode microplate reader (Tecan, Crailsheim, Germany). The IC_{50} values were calculated as mean values of three different repetitions.

2.7. Cell toxicity assay

The toxicity of the candidate drugs was investigated using a resazurin conversion assay (CellTiterBlue®, Promega, Mannheim, Germany). For Vero E6 cells, supernatants of previously plated cells were first replaced with 100 μL fresh medium for each sample. Then, 20 μL CellTiter-Blue® reagent (Promega) was added per well, and cells were incubated for 4 h at 37 °C with 5 % CO_2. Colorimetric analysis of treated cells was done with a Spark® 10 M multimode microplate reader (Tecan), detecting fluorescence with an excitation of 560 nm and an

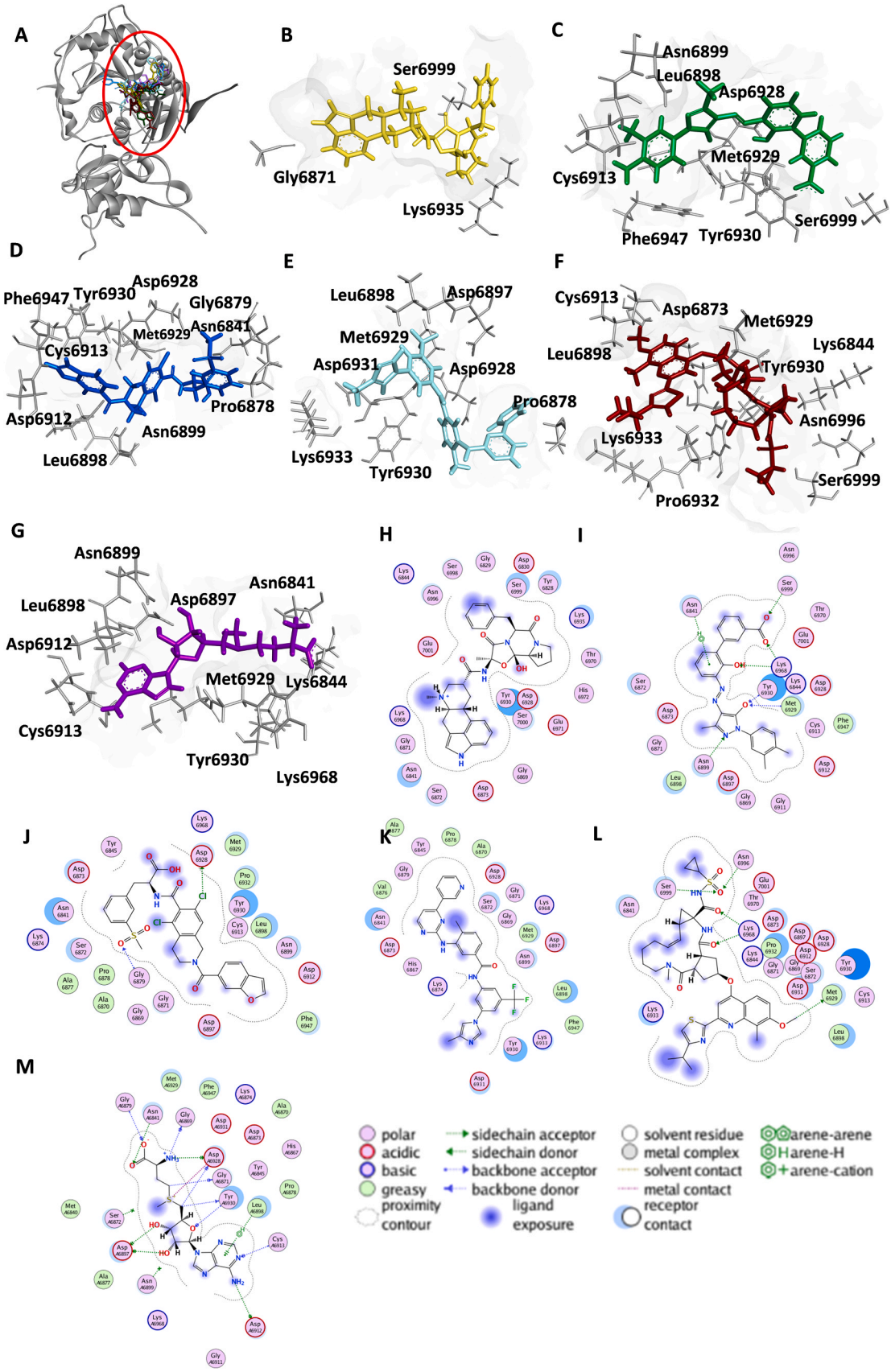

Fig. 3. MOE-based molecular docking of the selected candidates binding to the nsp16 methyltransferase of SARS-CoV-2 (PDB: 6W4H). (A) Binding of all candidates. Interactions of amino acid with (B) dihydroergotamine (gold); (C) eltrombopag (green); (D) lifitegrast (blue); (E) nilotinib (magenta); (F) simeprevir (red), and (G) SAM (purple). (H-M) are 2D views of (B-G), respectively. Images were created using Discovery Studio Visualizer.

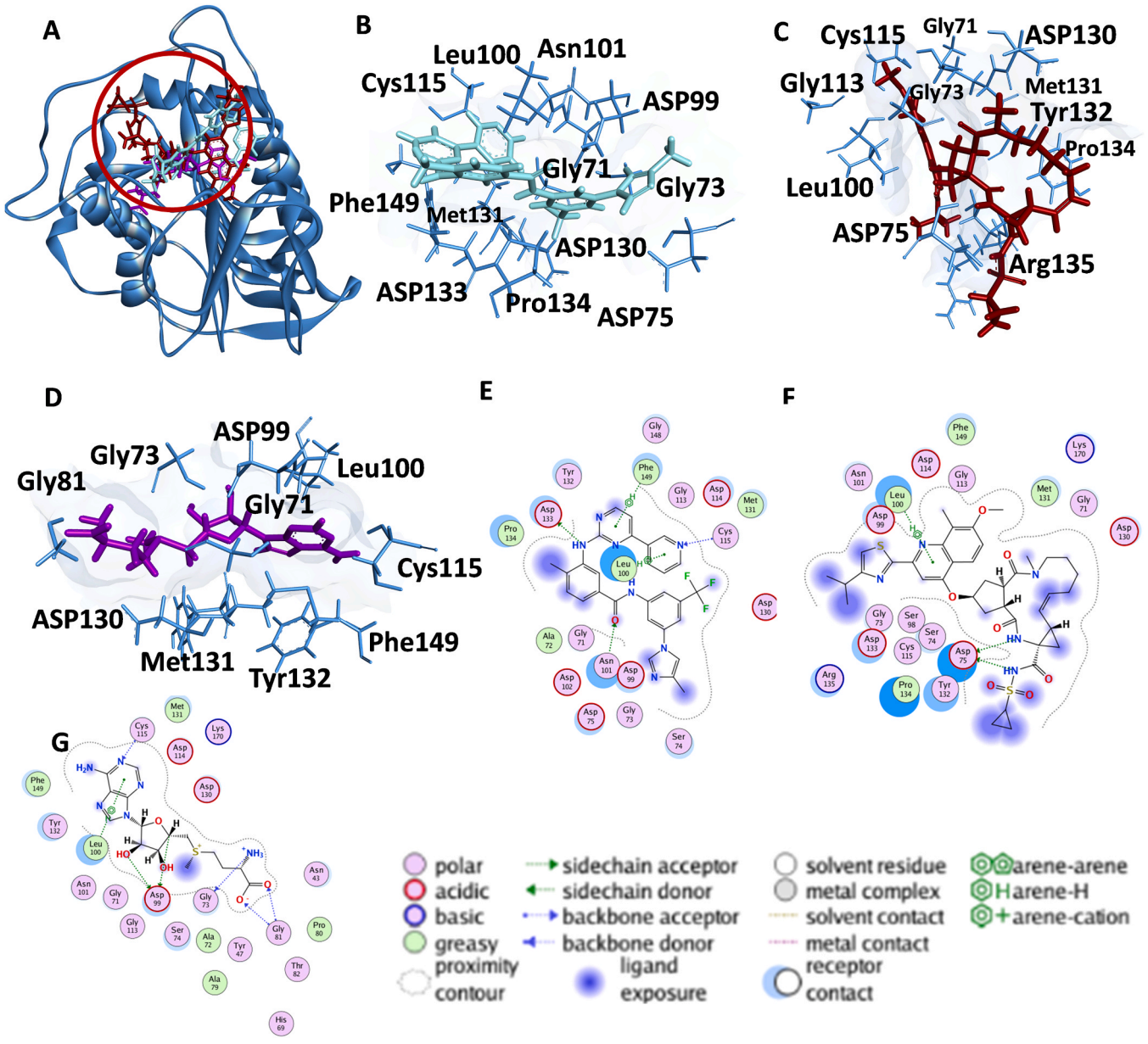

Fig. 4. MOE-based molecular docking of the selected candidates binding to the nsp16 methyltransferase of SARS-CoV-1 (PDB: 3R24). (A) Binding of all candidates. Interactions of amino acids with (B) nilotinib (magenta), (C) simeprevir (red), and (D) SAM (purple). (E-G) are 2D views of (B-D), respectively. Images were created using Discovery Studio Visualizer.

emission at 590 nm. The human diploid lung fibroblasts cell line MRC-5 was provided by Dr. rer. nat. Sebastian Zahnreich (Department of Radiation Oncology and Radiation Therapy, University Medical Center of the Johannes Gutenberg University, Mainz, Germany). As previously described [26], the cells were seeded in 96-well plates (20×10^5 cells/well) and incubated overnight. After the incubation period, treatment was added. The five candidates were tested in 10 concentrations each ranging between 0.3 and 100 μM. The plates were incubated for 24 h at 37 °C and 5 % CO_2. Again, 20 μL of 0.01 % resazurin solution was added to each well and incubated for 4 h. The plates were read at 550/590 nm using an Infinite® M200 Pro plate reader (Tecan). The IC_{50} values were calculated as the mean of three independent experiments, each containing six replicates.

2.8. Molecular dynamics simulations

For the MD simulation, the best docking pose of each compound with the nsp16-nsp10 complex was used. These poses were obtained through molecular docking using MOE and chosen based on the docking score. Initially, the complexes underwent energy minimization and protonation using MOE's QuickPrep function, employing the Amber10:EHT forcefield. The MD simulation files were also generated using MOE. First, the system underwent energy minimization, followed by heating to 300 K over 100 ps. Subsequently, an equilibration phase was conducted, including an NVT ensemble for 100 ps at 300 K and an NPT ensemble for 200 ps at 300 K and 1 atm pressure. This was followed by the production phase of 50 ns with a timestep of 2 fs. A frame was recorded every 10 ps. The simulation was performed using Nanoscale Molecular Dynamics (NAMD) 2.14 software [27], and each run was repeated three times independently. Trajectory analysis was carried out using Visual Molecular Dynamics (VMD) version 1.9.4a53 [28], which involved the calculation of RMSD, RMSF, and the occupancy of amino acids in contact. For the occupancy analysis, residue contacts with the compounds were monitored over 5,000 frames using a 3.5 Å cutoff to

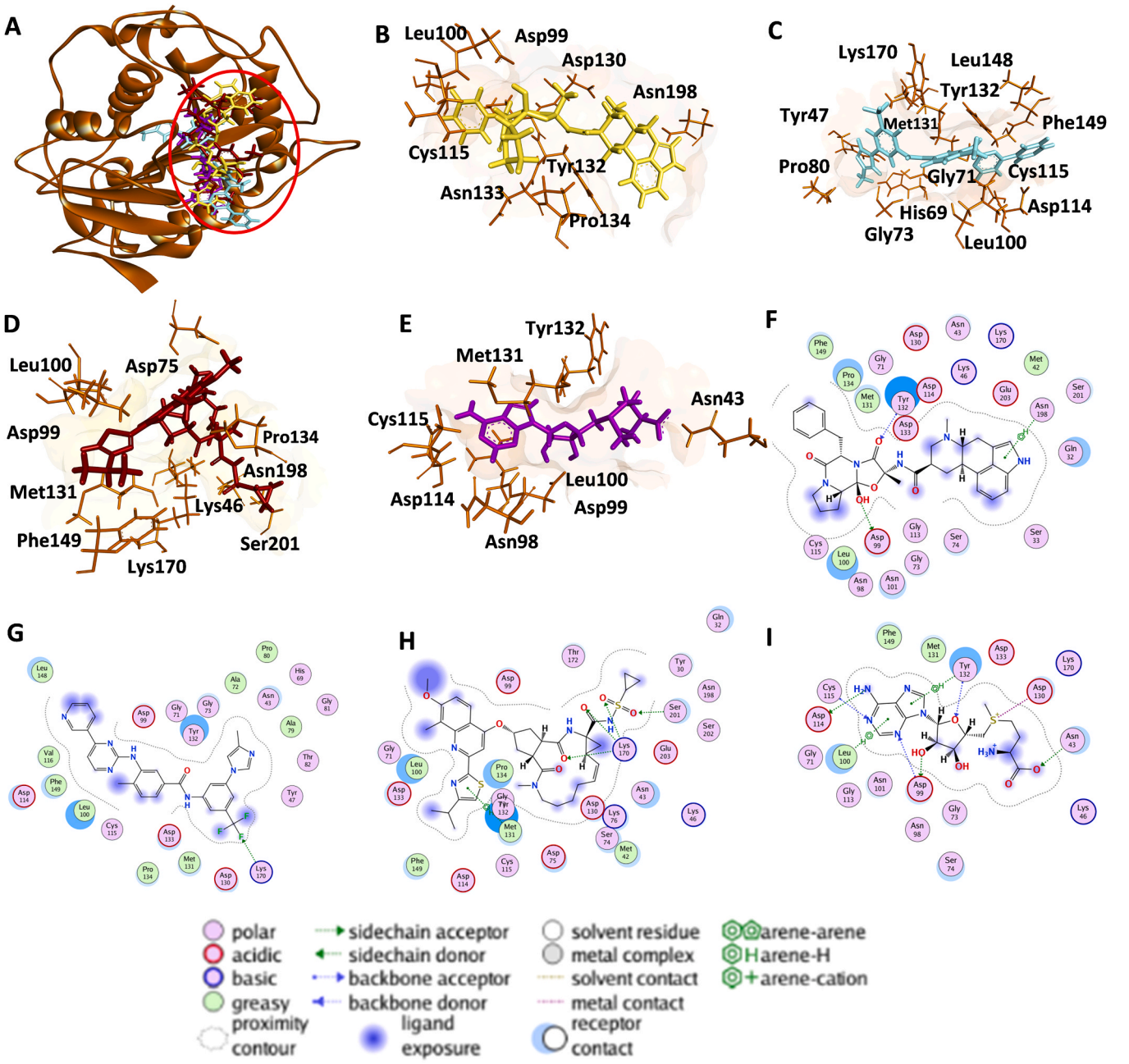

Fig. 5. MOE-based molecular docking of the selected candidates bound to the nsp16 methyltransferase of MERS-CoV (PDB: 5YN6). (A) Binding of all candidates. Interactions of amino acids with (B) dihydroergotamine (gold), (C) nilotinib (magenta), (D) simeprevir (red), and (E) SAM (purple). (F-I) are 2D views of (B-E), respectively. Images were created using Discovery Studio Visualizer.

identify the most frequently interacting amino acids with the help of the VMD timeline plugin.

3. Results

3.1. Virtual drug screening and molecular docking

First, PyRx-based virtual drug screening using 1577 FDA-approved drugs was performed. The 10 ligands that showed the highest binding affinities to all nsp16s of SARS-CoV-2, SARS-CoV-1, and MERS-CoV are listed in Table 1. The chemical structures of the selected ligands, together with the natural substrate S-adenosyl methionine (SAM), are shown in Fig. 1.

In order to visualize the interactions in the binding pocket, all candidates were subjected to molecular docking using MOE against SARS-CoV-2 nsp16 proteins. The S-scores of candidates together with the natural substrate S-adenosyl methionine (SAM) are shown in Table 1.

3.2. Assessment of binding affinity using microscale thermophoresis

The binding between candidates and the labeled recombinant nsp16 proteins of SARS-CoV-2, SARS-CoV-1, and MERS-CoV was investigated using the sensitive microscale thermophoresis (MST) technique. A strong binding between SARS-CoV-2 nsp16 and nilotinib, lifitegrast, dihydroergotamine, eltrombopag, and simeprevir could be shown. Both nilotinib and simeprevir bound to nsp16 of all coronaviruses tested, suggesting their potential to be broad-spectrum coronavirus inhibitors.

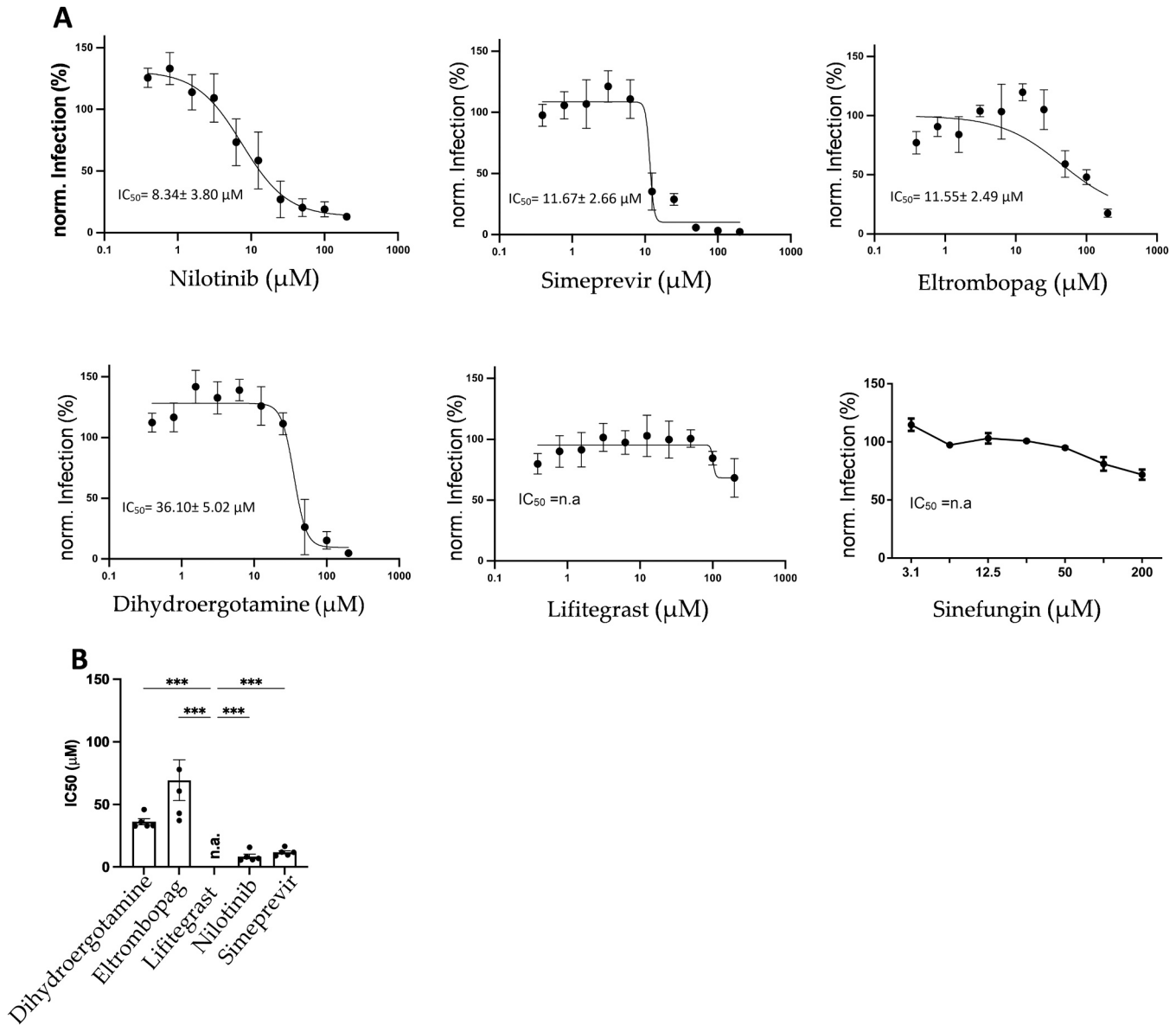

Fig. 6. Antiviral activity of candidate nsp16 inhibitors. (A) Vero E6 cells were infected with SARS-CoV-2 for 24 h in presence of different compound concentrations. Infection levels were quantified by in-cell ELISA and normalized to mock-treated control wells (infected but non-treated). Infection data were fitted with a four parameters inhibitor vs. response function (Y = bottom + (top-bottom)/(1 +(IC_{50}/X)^hillslope) using the statistics software GraphPad prism software. (B) Mean IC_{50} concentrations ± standard deviations were calculated from at least three independent titrations of each compound; *** p = 0.001–0.0001. The significance was assessed by ordinary one-way ANOVA. Calculated IC_{50} values for lifitegrast were disregarded since no significant antiviral effect was observed in the investigated concentration range.

The lowest K_d was 1.68 ± 0.44 µM for nilotinib bound to SARS-CoV-2 nsp16. The K_d values of all candidates bound to all tested nsp16s are shown in Table 2. The complete figures are provided in Fig. 2.

3.3. Interactions of the candidates with the nsp16 binding pocket of the three coronaviruses

Based on the MST findings, candidates showing strong binding to nsp16 of SARS-CoV-1 and MERS-CoV were docked to the substrate binding pocket of each target protein. While PyRx provided a first screening step for potential binding partners, molecular docking with the same protein structures mentioned above was then performed for nsp16 of SARS-CoV-1 and MERS-CoV, applying MOE to give deeper insights into amino acids involved in the interactions. The binding affinities of all docked candidates were higher than SAM, the natural substrate of nsp16. Among the docked candidates, simeprevir showed the highest binding affinity towards SARS-CoV-2, SARS-CoV-1 nsp16, and MERS-CoV nsp16 (Table 3). The interactions of the candidates with the amino acids in the nsp16-binding pocket of the target proteins are shown in Figs. 3–5. The results of docking for all nsp16s of SARS-CoV-2, SARS-CoV-1, and MERS-CoV are shown in Table 3.

3.4. SARS-CoV-2 inhibition in cell culture

The five drugs with strong binding to nsp16 of SARS-CoV-2 *in silico* and in MST assays were tested against the virus in cell culture. For that purpose, cells were infected in the presence of one of the selected compounds each compound for 24 h and then subjected to an in-cell ELISA as recently described [25]. Four of the five compounds inhibited viral replication at micromolar concentrations. Nilotinib showed the lowest IC_{50} among the candidates (8.34 ± 3.80 µM). followed by eltrombopag (11.55 ± 2.49 µM), simeprevir (11.67 ± 2.66 µM) and

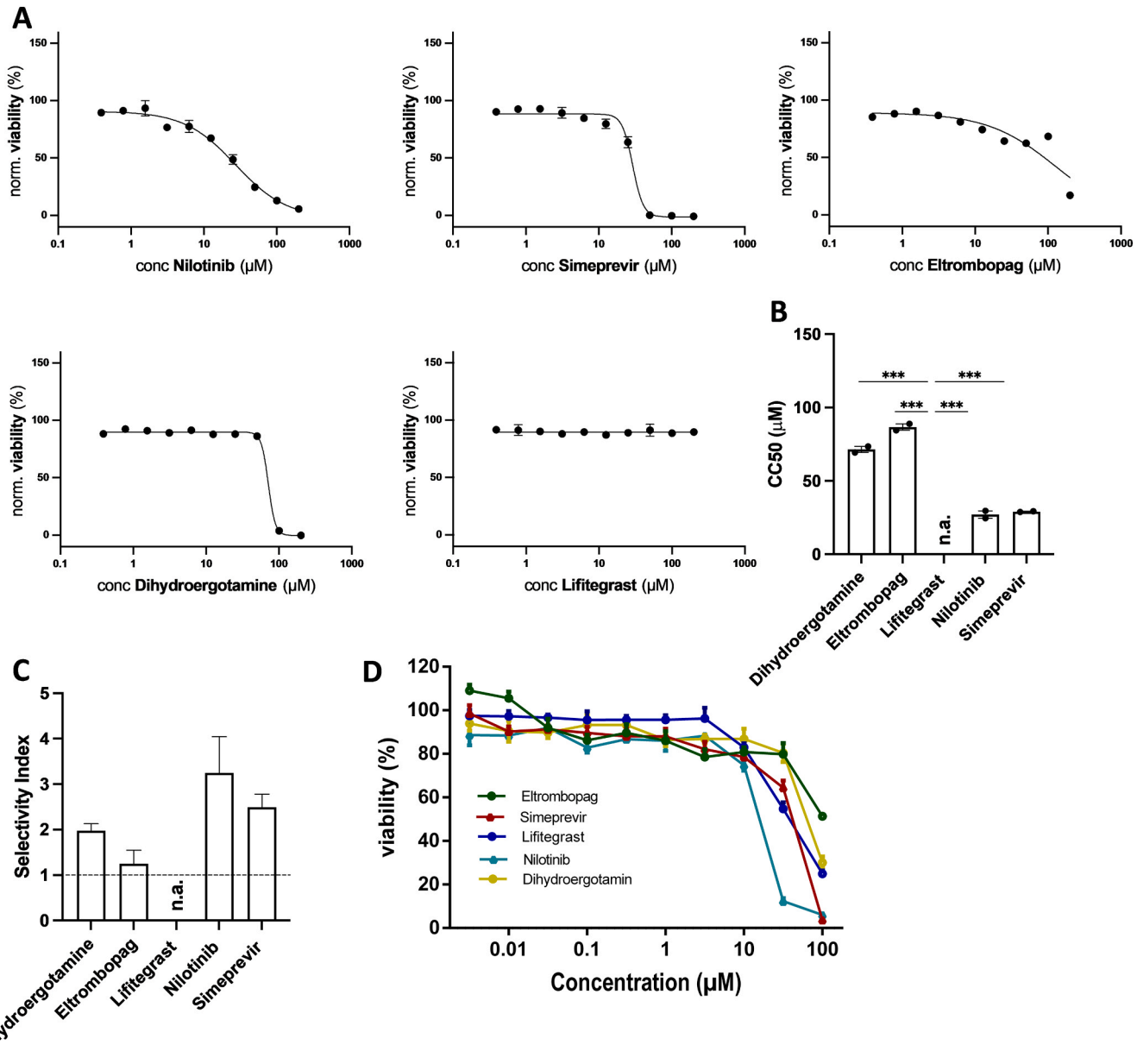

Fig. 7. Cytotoxicity of candidate nsp16 inhibitors in Vero E6 cells. (A) Cells were treated for 24 h with nsp16 inhibitors at different concentrations and then subjected to cell titer blue analysis. Data were fitted with a four parameters inhibitor *vs.* response function (Y = bottom + (top-bottom)/(1 +(IC_{50}/X)^hillslope) using the statistics software GraphPad prism. (B) Mean CC_{50} concentrations are shown with SD and were calculated from at least two independent titrations of each compound. * p = 0.01–0.05; *** p = 0.001–0.0001. The significance was assessed by ordinary one-way ANOVA. C. Selectivity Index(SI) = CC_{50}/IC_{50}. Calculated CC_{50} values for lifitegrast were disregarded since no significant toxic effect was observed in the investigated concentration range. (D) Dose-response curves of the candidate nsp16 inhibitors. Cell viability assays were performed using MRC-5 cells. The data represented three independent experiments' mean values ± standard deviations.

dihydroergotamine (36.10 ± 5.02 μM). Lifitegrast had a negligible activity against the virus in cell culture (Fig. 6).

3.5. Cytotoxicity of the candidates to Vero E6 cells

To further evaluate the activity of the identified candidate drugs, we compared their selectivity, *i.e.*, the inhibitory concentrations in SARS-CoV-2 *versus* the cytotoxicity in virus-infected cells. The cytotoxicity of the candidates was investigated using Vero E6 cells treated with the candidate compounds for 24 h. The least toxic candidate was eltrombopag, followed by dihydroergotamine, simeprevir, and nilotinib with IC_{50} values of 86.68, 71.44, 29.11, and 27.01 μM, respectively (Fig. 7A-C).

3.6. Toxicity of the candidates to MRC-5 cells

Human diploid MRC-5 lung fibroblasts were also used to assess the cytotoxicity of the candidates. Compared with the results in Vero E6 cells, the least toxic candidate was eltrombopag, followed by dihydroergotamine, simeprevir, and nilotinib with CC_{50} values of > 100, 62.73 ± 5.14, 39.87 ± 2.39, and 15.45 ± 0.59 μM, respectively (Fig. 7. **D**).

3.7. Validation of candidates-nsp16 binding using molecular dynamics simulations

Molecular Dynamics (MD) simulations were performed to study the flexibility and stability of nsp16-nsp10-compound complexes. Root mean square deviation (RMSD) values for four compounds were

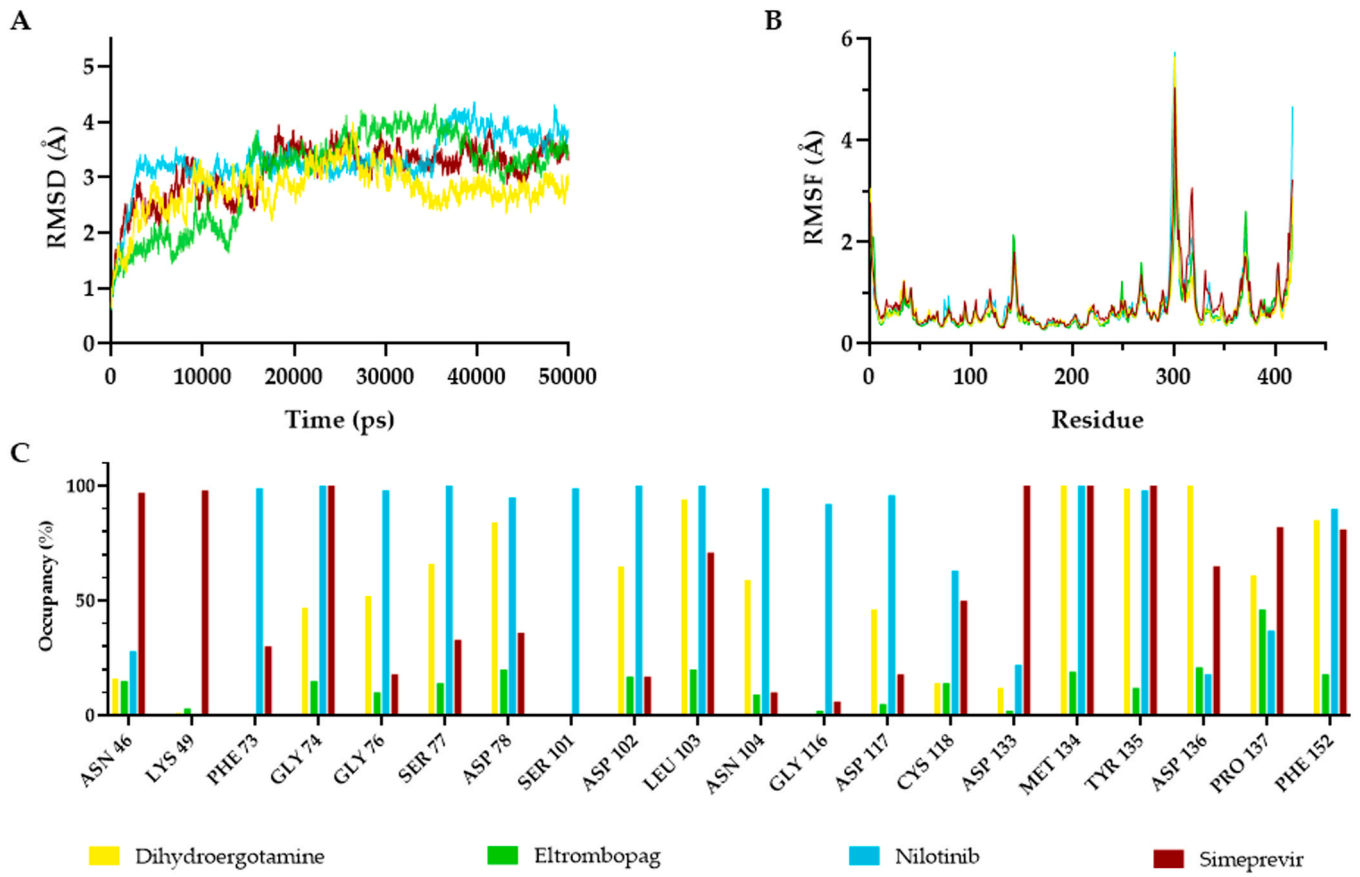

Fig. 8. Molecular dynamics simulations of nsp 16- nsp 10-compound Complexes over a 50,000 ps Simulation. (A) RMSD plots show the stability of the nsp16-nsp10-compound complexes. (B) RMSF values indicate the flexibility of specific residues within the protein-ligand complexes. (C) Occupancy analysis of the top 20 most frequently interacting amino acid residues, showing the percentage of time each residue was in contact with the compounds over 5000 frames using a 3.5 Å distance cutoff. The plots compare the dynamic behavior of nsp16-nsp10 in complex with four different compounds: Dihydroergotamine (yellow), Eltrombopag (green), Nilotinib (cyan), and Simeprevir (red).

analyzed over a 50 ns MD simulation (Fig. 8A). The simulation was performed in triplicates. The average RMSD values were 3.08 ± 0.49 Å for dihydroergotamine, 3.15 ± 0.19 Å for eltrombopag, 3.10 ± 0.22 Å for nilotinib, and 3.07 ± 0.30 Å for simeprevir. Dihydroergotamine showed the lowest average RMSD, which indicates a relatively stable binding conformation. In contrast, nilotinib showed the highest average RMSD, suggesting more conformational fluctuations. In particular, nilotinib exhibited a significant RMSD increase at approximately 35,000 ps, suggesting a conformational change during the MD simulation. After this deviation, the RMSD of nilotinib stabilized, indicating that a new steady state had been reached. Eltrombopag showed high fluctuations throughout the simulation, which suggests significant conformational flexibility. In contrast, simeprevir maintained a relatively stable RMSD for most of the simulation.

To investigate the flexibility of the residues in the nsp16-nsp10-compound complexes, the root mean square fluctuation (RMSF) was utilized (Fig. 8. B). The RMSF profiles for all four compounds showed similar trends, with increased flexibility observed in the region between residues 300 and 418. These residues are primarily part of nsp10. The highest flexibility was found near the terminus around residues 300 and 418. Notably, these flexible regions are outside the nsp16 binding pocket (approximately residues 50–150) where the compounds interact. While the overall RMSF patterns were similar across all compounds, minor deviations in the amplitudes could be observed. For example, nilotinib exhibited higher RMSF values around residues 75, 115, and 125 in the binding pocket. This suggests not only its influence on the protein's dynamics but also that nilotinib has a greater impact compared to the other tested compounds in these regions.

An occupancy analysis was performed to understand better how the tested compounds interact with the nsp16 binding pocket. This involved monitoring residue contacts over 5000 frames and calculating the occupancy to evaluate interaction frequency and stability. A 3.5 Å cutoff was used, and the 20 most frequently interacting amino acids were identified (Fig. 8C). Nilotinib showed nearly 100 % occupancy with various residues, such as PHE 73, GLY 74, and SER 77, which indicates a robust and consistent binding mode. MET 134 and TYR 135 exhibited high occupancy for all compounds except eltrombopag. This is consistent with eltrombopag's overall low occupancy and also correlated with its high RMSD fluctuations, which suggests weaker and less stable interactions between this compound and nsp16. Dihydroergotamine exhibited moderate occupancy with the highest values at residues 134–136, suggesting stable binding within specific regions of the pocket. Similarly, simeprevir displayed high occupancy at the same residues and ASN 46, LYS 49, and others. Overall, residues such as MET 134, TYR 135, and PHE 152 exhibited consistent interactions across most tested compounds.

4. Discussion

The first two human pathogenic coronaviruses discovered were 229E and OC43 in 1966 and 1967, respectively. After a long period of absence, another coronavirus was isolated in 2002. Afterwards, further novel coronaviruses emerged, culminating in a total of seven human pathogenic viruses, two of which posed significant public health threats during a span of 20 years [29]. Evolutionary molecular analysis of the reference genome of the latest coronavirus SARS-CoV-2 revealed that it

originates from mammals. Previous regional epidemics, such as SARS and MERS, were linked to viruses within the same phylogenetic group, all of which are from zoonotic origin. These findings imply that coronaviruses can spread between animals, including humans. Additionally, the recombination between different strains of the virus living in various host species can result in the rise of new variants of the coronavirus genome [30,31]. This highlights the urgent need for novel target-specific anti-coronaviral drugs with high efficacy, fewer side effects and lower costs.

The zoonotic nature of coronaviruses, as well as their mutative potential, provide significant challenges for targeting these viruses. The latter challenge may be overcome by targeting conserved fragments on the virus such as nsp16, which is essential for coronaviral replication [32]. Moreover, it is a highly conserved protein among the entire family with less mutative capability. It has been suggested in previous studies, that targeting nsp16 might provide candidates drugs which are effective against prior strains such as SARS-CoV and HCoV 229E, as well as MERS-CoV and PEDV which emerged at that time [12,33]. This hypothesis was verified many years later by other studies performed after the COVID-19 pandemic, particularly due to the distinctions between the viral methyltransferase and the human homolog CMTr1 [18,34,35]. Targeting a pocket in nsp16 may serve as a new approach for drug discovery against pan-coronavirus [36]. This approach was used to identify SS148 and WZ16, both of which are nsp16 inhibitors of all of the human coronaviruses, hence endorsing the potential for the creation of broad-spectrum nsp16 inhibitors [37].

The concept of pan-coronavirus inhibitors has been addressed at different levels of investigation including *in silico*, *in vitro*, and *in vivo* [38–41]. Different strategies have been used, including inhibiting virus entry into the cells, or inhibiting virus replication. Pan-inhibitors of virus entry were targeting either host cysteine proteases such as cathepsin L (CTSL) and calpain-1 (CAPN1) [42], viral spike protein [43], or Niemann-Pick C1 [44]. Other pan-inhibitors that target virus replication and translation include main pan-protease inhibitors [26,39], nsp16 pan-inhibitors [18], and nucleocapsid protein pan-inhibitors [45]. These afore-mentioned studies utilized different coronaviruses for investigation, including SARS-CoV-2, SARS-CoV, MERS-CoV, HCoV-NL63, HCoV-OC43, HCoV-229E, and HCoV-HKU1.

Considering there is no drug targeting nsp16 yet, we addressed this protein in order to identify potential pan-inhibitors for SARS-CoV-2, SARS-CoV-1, and MERS-CoV in the present study. We screened an FDA-approved library for pan-coronavirus inhibitors targeting nsp16 of the three coronaviruses. An added value of in silico analyses is that active drugs can be identified in a cost- and time-saving manner, thereby speeding up the drug discovery process [46]. Virtual drug screening has been established in the pharmaceutical industry since many years as a first step of drug discovery. The candidates identified by such bioinformatical techniques must then be validated with subsequent assays such as microscale thermophoresis and live virus inhibition assays.

In this study, the results of *in silico* investigation together with the binding assay using MST indicated that niloinib and simeprevir bound to all tested nsp16. Therefore, we suggest these candidates as potential pan-coronavirus inhibitors. Other candidates such as eltrombopag, lifitegrast, and dihydroergotamine showed binding mainly to nsp16 of SARS-CoV-2. Our *in silico* screening results are in line with previous results of our research group, that nilotinib, eltrombopag, lifitegrast, and dihydroergotamine bound to the substrate binding pocket of nsp16 of SARS-CoV-2 suggesting them as potential inhibitors for this protein [47].

Based on the *in silico* and MST binding assay results, we tested the candidates *in vitro* against SARS-CoV-2 using Vero E6 cells. Again, nilotinib was the strongest inhibitor followed by simeprevir, eltrombopag and dihydroergotamine. Here, as a positive control, we used the pan-methyltransferase inhibitor sinefungin which is widely used in nsp10–16 biochemical assays [48–51]. However, it has low inhibitory effect in cell culture-based assay due to its poor membrane permeability [52,53]. The previous reports for nilotinib activity as SARS-CoV-2 main protease inhibitor *in silico* and *in vitro* [37,54,55], in addition to its activity against SARS-CoV-1 and Ebola virus *in vitro* [56,57], together with our findings may stimulate further investigations on nilotinib as anti-coronavirus.

We performed MD simulation because it provides more insights into individual atomic motion than molecular docking [48,49]. Here, MD simulations showed that nilotinib exhibited the highest conformational flexibility among all drugs investigated with a structural shift followed by stabilization. This suggests a reorganization of its binding mode (Fig. 8A, supplementary videos). Furthermore, nilotinib showed dynamic interactions with regions in the SAM binding pocket. These fluctuations may indicate a more flexible and adaptable binding behaviour compared to the other tested compounds, which potentially influences its efficacy as a coronavirus inhibitor. Despite both simeprevir and eltrombopag having similar activity against SARS-CoV-2, the MST results showed that simepervir had the advantage that it bound to all tested nsp16 proteins suggesting it's potential to be a pan-coronavirus nsp16 inhibitor. Simepervir also maintained a relatively stable RMSD for most of the MD simulation. Our findings extend previous results showing that the hepatitis C virus protease-inhibitor simeprevir inhibited SARS-CoV-2. Different mechanisms of SARS-CoV-2 inhibition were previously reported, including inhibition of SARS-CoV-2 protease *in silico* [48,58] Simeprevir also inhibited SARS-CoV-2 dimerization of Nsp9 *in silico* [59], spike receptor-binding [60] and RdRp and M^{pro} proteins of SARS-CoV-2 [61]. Simeprevir has synergistic effect with remdesivir in inhibiting SARS-CoV-2 replication [62,63].

In the present work, dihydroergotamine bound to nsp16 of both SARS-CoV-2 and MERS-CoV but not nsp16 of SARS-CoV-1, whereas eltrombopag only bound to nsp16 of SARS-CoV-2 suggesting both may not have a sufficient potential as pan- nsp16 inhibitors. Nevertheless, they could act as possible SARS-CoV-2 inhibitors. The *in vitro* investigation showed that the IC_{50} values were 11.55 and 36.1 μM for eltrombopag and dihydroergotamine, respectively. Our MD simulations revealed the lowest average RMSD values for dihydroergotamine, which suggests a stable interaction within the binding pocket. By contrast, eltrombopag showed higher fluctuation and flexibility. Notably, both drugs inhibited SARS-CoV-2 proteases and spike protein *in silico* [64–67], as well as in cell-based assays in which the authors suggested further research to investigate the target of this molecule [68,69].

Here, we identified both nilotinib and simeprevir as possible pan-nsp16 inhibitors for SARS-CoV-2, SARS-CoV-1 and MERS-CoV. Simeprevir is a well-tolerated antiviral drug with less side effects than nilotinib [70]. On the other hand, the price of oral capsules of simepriver 150 mg is around $23,000 for a supply of 28 capsules whereas the supply of an equivalent quantity of 150 mg nilotinib capsules cost only around $5300 [71,72]. Sinceeconomic aspects play an important role for clinical applicability, this is a significant difference worth considering. As a matter of fact, some of the approved drugs on the market are still expensive but may become more affordable upon widespread use in pandemics, or if competitor drugs enter the market. We think it is ethically justified to use expensive drugs for diseases where other drugs are not yet available, and if there is significant scientific indication [73,74].

So far, both drugs have reasonable safety profiles. In the current investigation, nilotinib was more effective than simeprevir *in vitro,* as well as being more cost-effective. Therefore, we advocate for more research on nilotinib as an antiviral agent, evaluating its efficacy besides simepriver against clinical isolates of several coronaviruses. Taking into consideration that drugs such as PCG vaccine, rituximab, methotrexate, thalidomide and hydroxyurea have both oncological and non-oncological clinical applications.

5. Conclusions

Using a drug repurposing concept with in silico and in vitro techniques, we provided four promising candidates that target various coronaviruses. Broad-spectrum coronaviral inhibitors could be a powerful tool in targeting novel coronaviruses and co-infection with different viruses. Broad-spectrum or pan-inhibitors may also gain relevance in the future, if new coronaviruses emerge causing new epidemics or pandemics. Such drugs may also have great value in addressing not only wild-type coronaviruses but also their mutant variants. While their selectivity and specificity require further investigation, economic aspects should also be considered.

CRediT authorship contribution statement

Axel Guthart: Writing – original draft, Software, Methodology. **Kathrin Sutter:** Writing – original draft, Methodology. **Sara Abdelfatah:** Conceptualization. **Nasim Shahhamzehei:** Methodology. **Thomas Efferth:** Writing – review & editing, Supervision, Conceptualization. **Hannah S. Schwarzer-Sperber:** Writing – original draft, Methodology. **Roland Schwarzer:** Writing – original draft, Methodology. **Ejlal A. Omer:** Writing – original draft, Software, Methodology, Formal analysis, Data curation.

Institutional Review Board Statement

Not applicable. Informed Consent Statement: Not applicable. Data Availability Statement: Data is contained within the article.

Funding

This study was funded by a donation from Marc Strobel, CVC Capital Partners, Frankfurt a. M., Germany and CVC Philanthropy, Jersey.

Declaration of Competing Interest

The authors declare the following financial interests/personal relationships which may be considered as potential competing interests: Ejlal A. Omer reports financial support was provided by German Academic Exchange Service. If there are other authors, they declare that they have no known competing financial interests or personal relationships that could have appeared to influence the work reported in this paper.

Acknowledgement

We are grateful for the Ph.D. stipend from the German Academic Exchange Service (DAAD). We also acknowledge Dr. rer. nat. Sebastian Zahnreich (Department of Radiation Oncology and Radiation Therapy, University Medical Center of the Johannes Gutenberg University, Mainz, Germany) for donating the MRC-5 cells. We also acknowledge Ms. Lara J. Friedrich (Department of Pharmaceutical Biology, Institute of Pharmaceutical and Biomedical Sciences, Johannes Gutenberg University).

Appendix A. Supporting information

Supplementary data associated with this article can be found in the online version at doi:10.1016/j.biopha.2025.118246.

References

[1] M. Shi, X.-D. Lin, J.-H. Tian, L.-J. Chen, X. Chen, C.-X. Li, X.-C. Qin, J. Li, J.-P. Cao, J.-S. Eden, J. Buchmann, W. Wang, J. Xu, E.C. Holmes, Y.-Z. Zhang, Redefining the invertebrate RNA virosphere, Nature 540 (2016) 539–543, https://doi.org/10.1038/nature20167.

[2] A. Zapatero Gaviria, R. Barba Martin, What do we know about the origin of COVID-19 three years later? Revista Clínica Española (English Edition) 223 (2023) 240–243, https://doi.org/10.1016/j.rceng.2023.02.010.

[3] B. Hu, H. Guo, P. Zhou, Z.-L. Shi, Characteristics of SARS-CoV-2 and COVID-19, Nat. Rev. Microbiol 19 (2021) 141–154, https://doi.org/10.1038/s41579-020-00459-7.

[4] WHO Coronavirus (COVID-19) Dashboard, (n.d.). ⟨https://covid19.who.int⟩ (accessed September 21, 2023).

[5] A.M. Carabelli, T.P. Peacock, L.G. Thorne, W.T. Harvey, J. Hughes, T.I. de Silva, S. J. Peacock, W.S. Barclay, T.I. de Silva, G.J. Towers, D.L. Robertson, SARS-CoV-2 variant biology: immune escape, transmission and fitness, Nat. Rev. Microbiol. 21 (2023) 162–177, https://doi.org/10.1038/s41579-022-00841-7.

[6] S. Steiner, A. Kratzel, G.T. Barut, R.M. Lang, E. Aguiar Moreira, L. Thomann, J. N. Kelly, V. Thiel, SARS-CoV-2 biology and host interactions, Nat. Rev. Microbiol. (2024) 1–20, https://doi.org/10.1038/s41579-023-01003-z.

[7] S. Krishnamoorthy, B. Swain, R.S. Verma, S.S. Gunthe, SARS-CoV, MERS-CoV, and 2019-nCoV viruses: an overview of origin, evolution, and genetic variations, VirusDis 31 (2020) 411–423, https://doi.org/10.1007/s13337-020-00632-9.

[8] E.J. Snijder, E. Decroly, J. Ziebuhr, The nonstructural proteins directing coronavirus RNA synthesis and processing, Adv. Virus Res. 96 (2016) 59–126, https://doi.org/10.1016/bs.aivir.2016.08.008.

[9] Y.-H. Li, C.-Y. Hu, N.-P. Wu, H.-P. Yao, L.-J. Li, Molecular Characteristics, functions, and related pathogenicity of MERS-CoV proteins, Engineering 5 (2019) 940–947, https://doi.org/10.1016/j.eng.2018.11.035.

[10] M. Bartlam, H. Yang, Z. Rao, Structural insights into SARS coronavirus proteins, Curr. Opin. Struct. Biol. 15 (2005) 664–672, https://doi.org/10.1016/j.sbi.2005.10.004.

[11] M. Sevajol, L. Subissi, E. Decroly, B. Canard, I. Imbert, Insights into RNA synthesis, capping, and proofreading mechanisms of SARS-coronavirus, Virus Res. 194 (2014) 90–99, https://doi.org/10.1016/j.virusres.2014.10.008.

[12] V.D. Menachery, K. Debbink, R.S. Baric, Coronavirus non-structural protein 16: Evasion, attenuation, and possible treatments, Virus Res. 194 (2014) 191–199, https://doi.org/10.1016/j.virusres.2014.09.009.

[13] C. Schindewolf, V.D. Menachery, Coronavirus 2′-O-methyltransferase: a promising therapeutic target, Virus Res 336 (2023) 199211, https://doi.org/10.1016/j.virusres.2023.199211.

[14] M.H. Abbasian, M. Mahmanzar, K. Rahimian, B. Mahdavi, S. Tokhanbigli, B. Moradi, M.M. Sisakht, Y. Deng, Global landscape of SARS-CoV-2 mutations and conserved regions, J. Transl. Med. 21 (2023) 152, https://doi.org/10.1186/s12967-023-03996-w.

[15] S. Daffis, K.J. Szretter, J. Schriewer, J. Li, S. Youn, J. Errett, T.-Y. Lin, S. Schneller, R. Zust, H. Dong, V. Thiel, G.C. Sen, V. Fensterl, W.B. Klimstra, T.C. Pierson, R. M. Buller, M. Gale Jr, P.-Y. Shi, M.S. Diamond, 2′-O methylation of the viral mRNA cap evades host restriction by IFIT family members, Nature 468 (2010) 452–456, https://doi.org/10.1038/nature09489.

[16] E. Decroly, F. Ferron, J. Lescar, B. Canard, Conventional and unconventional mechanisms for capping viral mRNA, Nat. Rev. Microbiol. 10 (2012) 51–65, https://doi.org/10.1038/nrmicro2675.

[17] V.D. Menachery, L.E. Gralinski, H.D. Mitchell, K.H. Dinnon, S.R. Leist, B.L. Yount, R.L. Graham, E.T. McAnarney, K.G. Stratton, A.S. Cockrell, K. Debbink, A.C. Sims, K.M. Waters, R.S. Baric, Middle East respiratory syndrome coronavirus nonstructural protein 16 is necessary for interferon resistance and viral pathogenesis, MSphere 2 (2017), https://doi.org/10.1128/msphere.00346-17.

[18] E.A. Omer, S. Abdelfatah, M. Riedl, C. Meesters, A. Hildebrandt, T. Efferth, Coronavirus inhibitors targeting nsp16, Molecules 28 (2023) 988, https://doi.org/10.3390/molecules28030988.

[19] S. Pushpakom, F. Iorio, P.A. Eyers, K.J. Escott, S. Hopper, A. Wells, A. Doig, T. Guilliams, J. Latimer, C. McNamee, A. Norris, P. Sanseau, D. Cavalla, M. Pirmohamed, Drug repurposing: progress, challenges and recommendations, Nat. Rev. Drug Discov. 18 (2019) 41–58, https://doi.org/10.1038/nrd.2018.168.

[20] J. Dinić, T. Efferth, A.T. García-Sosa, J. Grahovac, J.M. Padrón, I. Pajeva, F. Rizzolio, S. Saponara, G. Spengler, I. Tsakovska, Repurposing old drugs to fight multidrug resistant cancers, Drug Resist Updat 52 (2020) 100713, https://doi.org/10.1016/j.drup.2020.100713.

[21] M.A. Bakowski, N. Beutler, K.C. Wolff, M.G. Kirkpatrick, E. Chen, T.-T.H. Nguyen, L. Riva, N. Shaabani, M. Parren, J. Ricketts, A.K. Gupta, K. Pan, P. Kuo, M. Fuller, E. Garcia, J.R. Teijaro, L. Yang, D. Sahoo, V. Chi, E. Huang, N. Vargas, A.J. Roberts, S. Das, P. Ghosh, A.K. Woods, S.B. Joseph, M.V. Hull, P.G. Schultz, D.R. Burton, A. K. Chatterjee, C.W. McNamara, T.F. Rogers, Drug repurposing screens identify chemical entities for the development of COVID-19 interventions, Nat. Commun. 12 (2021) 3309, https://doi.org/10.1038/s41467-021-23328-0.

[22] A.I. Graul, L. Sorbera, P. Pina, M. Tell, E. Cruces, E. Rosa, M. Stringer, R. Castañer, L. Revel, The Year's New Drugs & Biologics - 2009, Drug News Perspect. 23 (2010) 7–36, https://doi.org/10.1358/dnp.2010.23.1.1440373.

[23] N. Krishnamurthy, A.A. Grimshaw, S.A. Axson, S.H. Choe, J.E. Miller, Drug repurposing: a systematic review on root causes, barriers and facilitators, BMC Health Serv. Res. 22 (2022) 970, https://doi.org/10.1186/s12913-022-08272-z.

[24] C.S. Heilingloh, U.W. Aufderhorst, L. Schipper, U. Dittmer, O. Witzke, D. Yang, X. Zheng, K. Sutter, M. Trilling, M. Alt, E. Steinmann, A. Krawczyk, Susceptibility of SARS-CoV-2 to UV irradiation, Am. J. Infect. Control 48 (2020) 1273–1275, https://doi.org/10.1016/j.ajic.2020.07.031.

[25] L. Schöler, V.T.K. Le-Trilling, M. Eilbrecht, D. Mennerich, O.E. Anastasiou, A. Krawczyk, A. Herrmann, U. Dittmer, M. Trilling, A novel in-cell ELISA assay allows rapid and automated quantification of SARS-CoV-2 to analyze neutralizing antibodies and antiviral compounds, Front Immunol. 11 (2020) 573526, https://doi.org/10.3389/fimmu.2020.573526.

[26] N. Shahhamzehei, S. Abdelfatah, T. Efferth, In silico and in vitro identification of pan-coronaviral main protease inhibitors from a large natural product library, Pharmaceuticals 15 (2022) 308, https://doi.org/10.3390/ph15030308.
[27] J.C. Phillips, R. Braun, W. Wang, J. Gumbart, E. Tajkhorshid, E. Villa, C. Chipot, R. D. Skeel, L. Kalé, K. Schulten, Scalable molecular dynamics with NAMD, J. Comput. Chem. 26 (2005) 1781–1802, https://doi.org/10.1002/jcc.20289.
[28] W. Humphrey, A. Dalke, K. Schulten, VMD: visual molecular dynamics, J. Mol. Graph. 14 (1996) 33–38, https://doi.org/10.1016/0263-7855(96)00018-5.
[29] G. Tang, Z. Liu, D. Chen, Human coronaviruses: origin, host and receptor, J. Clin. Virol. 155 (2022) 105246, https://doi.org/10.1016/j.jcv.2022.105246.
[30] D. Singh, S.V. Yi, On the origin and evolution of SARS-CoV-2, Exp. Mol. Med 53 (2021) 537–547, https://doi.org/10.1038/s12276-021-00604-z.
[31] P.V. Markov, M. Ghafari, M. Beer, K. Lythgoe, P. Simmonds, N.I. Stilianakis, A. Katzourakis, The evolution of SARS-CoV-2, Nat. Rev. Microbiol. 21 (2023) 361–379, https://doi.org/10.1038/s41579-023-00878-2.
[32] C. Schindewolf, K. Lokugamage, M.N. Vu, B.A. Johnson, D. Scharton, J.A. Plante, B. Kalveram, P.A. Crocquet-Valdes, S. Sotcheff, E. Jaworski, R.E. Alvarado, K. Debbink, M.D. Daugherty, S.C. Weaver, A.L. Routh, D.H. Walker, K.S. Plante, V. D. Menachery, SARS-CoV-2 uses nonstructural protein 16 to evade restriction by IFIT1 and IFIT3, J. Virol. 97 (2023) e01532-22, https://doi.org/10.1128/jvi.01532-22.
[33] C.C. Melo-Filho, T. Bobrowski, H.-J. Martin, Z. Sessions, K.I. Popov, N.J. Moorman, R.S. Baric, E.N. Muratov, A. Tropsha, Conserved coronavirus proteins as targets of broad-spectrum antivirals, Antivir. Res. 204 (2022) 105360, https://doi.org/10.1016/j.antiviral.2022.105360.
[34] L.-J. Chang, T.-H. Chen, NSP16 2′-O-MTase in coronavirus pathogenesis: possible prevention and treatments strategies, Viruses 13 (2021) 538, https://doi.org/10.3390/v13040538.
[35] N. Vithani, M.D. Ward, M.I. Zimmerman, B. Novak, J.H. Borowsky, S. Singh, G. R. Bowman, SARS-CoV-2 Nsp16 activation mechanism and a cryptic pocket with pan-coronavirus antiviral potential, BioRxiv (2020), https://doi.org/10.1101/2020.12.10.420109.
[36] N.L. Inniss, J. Kozic, F. Li, M. Rosas-Lemus, G. Minasov, J. Rybáček, Y. Zhu, R. Pohl, L. Shuvalova, L. Rulíšek, J.S. Brunzelle, L. Bednárová, M. Štefek, J. M. Kormaník, E. Andris, J. Šebestík, A.S.M. Li, P.J. Brown, U. Schmitz, K. Saikatendu, E. Chang, R. Nencka, M. Vedadi, K.J.F. Satchell, Discovery of a druggable, cryptic pocket in SARS-CoV-2 nsp16 using allosteric inhibitors, ACS Infect. Dis. 9 (2023) 1918–1931, https://doi.org/10.1021/acsinfecdis.3c00203.
[37] F. Li, P. Ghiabi, T. Hajian, M. Klima, A.S.M. Li, A. Khalili Yazdi, I. Chau, P. Loppnau, M. Kutera, A. Seitova, A. Bolotokova, A. Hutchinson, S. Perveen, E. Boura, M. Vedadi, SS148 and WZ16 inhibit the activities of nsp10-nsp16 complexes from all seven human pathogenic coronaviruses, Biochim. Biophys. Acta (BBA) Gen. Subj. 1867 (2023) 130319, https://doi.org/10.1016/j.bbagen.2023.130319.
[38] Ş. Adem, V. Eyupoglu, I. Sarfraz, A. Rasul, A.F. Zahoor, M. Ali, M. Abdalla, I. M. Ibrahim, A.A. Elfiky, Caffeic acid derivatives (CAFDs) as inhibitors of SARS-CoV-2: CAFDs-based functional foods as a potential alternative approach to combat COVID-19, Phytomedicine 85 (2021) 153310, https://doi.org/10.1016/j.phymed.2020.153310.
[39] J. Zhang, L. Zhao, Y. Bai, S. Li, M. Zhang, B. Wei, X. Wang, Y. Xue, L. Li, G. Ma, Y. Tang, X. Wang, An ascidian *Polycarpa aurata*-derived pan-inhibitor against coronaviruses targeting Mpro, Bioorg. Med. Chem. Lett. 103 (2024) 129706, https://doi.org/10.1016/j.bmcl.2024.129706.
[40] J. Gao, C. Cao, M. Shi, S. Hong, S. Guo, J. Li, T. Liang, P. Song, R. Xu, N. Li, Kaempferol inhibits SARS-CoV-2 invasion by impairing heptad repeats-mediated viral fusion, Phytomedicine 118 (2023) 154942, https://doi.org/10.1016/j.phymed.2023.154942.
[41] W. Wang, W. Li, Z. Wen, C. Wang, W. Liu, Y. Zhang, J. Liu, T. Ding, L. Shuai, G. Zhong, Z. Bu, L. Qu, M. Ren, F. Li, Gossypol broadly inhibits coronaviruses by targeting RNA-dependent RNA polymerases, Adv. Sci. 9 (2022) 2203499, https://doi.org/10.1002/advs.202203499.
[42] X. Xie, Q. Lan, J. Zhao, S. Zhang, L. Liu, Y. Zhang, W. Xu, M. Shao, J. Peng, S. Xia, Y. Zhu, K. Zhang, X. Zhang, R. Zhang, J. Li, W. Dai, Z. Ge, S. Hu, C. Yu, J. Wang, D. Ma, M. Zheng, H. Yang, G. Xiao, Z. Rao, L. Lu, L. Zhang, F. Bai, Y. Zhao, S. Jiang, H. Liu, Structure-based design of pan-coronavirus inhibitors targeting host cathepsin L and calpain-1, Sig Transduct. Target Ther. 9 (2024) 1–14, https://doi.org/10.1038/s41392-024-01758-8.
[43] H. Feng, L. Yang, H. Yang, D. Cheng, M. Li, E. Song, T. Xu, A cardiotoxicity-eliminated ACE2 variant as a pan-inhibitor against coronavirus cell invasion, Mol. Ther. 32 (2024) 218–226, https://doi.org/10.1016/j.ymthe.2023.11.019.
[44] I. Khan, S. Li, L. Tao, C. Wang, B. Ye, H. Li, X. Liu, I. Ahmad, W. Su, G. Zhong, Z. Wen, J. Wang, R.-H. Hua, A. Ma, J. Liang, X.-P. Wan, Z.-G. Bu, Y.-H. Zheng, Tubeimosides are pan-coronavirus and filovirus inhibitors that can block their fusion protein binding to Niemann-Pick C1, Nat. Commun. 15 (2024) 162, https://doi.org/10.1038/s41467-023-44504-4.
[45] A. Pohler, S. Abdelfatah, M. Riedl, C. Meesters, A. Hildebrandt, T. Efferth, Potential coronaviral inhibitors of the nucleocapsid protein identified in silico and in vitro from a large natural product library, Pharmaceuticals 15 (2022) 1046, https://doi.org/10.3390/ph15091046.
[46] A. Lavecchia, C.Di Giovanni, Virtual screening strategies in drug discovery: a critical review, Curr. Med. Chem. 20 (2013) 2839–2860, https://doi.org/10.2174/09298673113209990001.
[47] O. Kadioglu, M. Saeed, H.J. Greten, T. Efferth, Identification of novel compounds against three targets of SARS CoV-2 coronavirus by combined virtual screening and supervised machine learning, Comput. Biol. Med. 133 (2021) 104359, https://doi.org/10.1016/j.compbiomed.2021.104359.
[48] A. Khalili Yazdi, F. Li, K. Devkota, S. Perveen, P. Ghiabi, T. Hajian, A. Bolotokova, M. Vedadi, A High-Throughput Radioactivity-Based Assay for Screening SARS-CoV-2 nsp10-nsp16 Complex, Slas Discovery: Advancing Science Drug Discovery 26 (2021) 757–765, https://doi.org/10.1177/24725552211008863.
[49] S. Perveen, A. Khalili Yazdi, K. Devkota, F. Li, P. Ghiabi, T. Hajian, P. Loppnau, A. Bolotokova, M. Vedadi, A high-throughput RNA displacement assay for screening SARS-CoV-2 nsp10-nsp16 complex toward developing therapeutics for COVID-19, SLAS Discov. 26 (2021) 620–627, https://doi.org/10.1177/2472555220985040.
[50] K. Devkota, M. Schapira, S. Perveen, A. Khalili Yazdi, F. Li, I. Chau, P. Ghiabi, T. Hajian, P. Loppnau, A. Bolotokova, K.J.F. Satchell, K. Wang, D. Li, J. Liu, D. Smil, M. Luo, J. Jin, P.V. Fish, P.J. Brown, M. Vedadi, Probing the SAM binding site of SARS-CoV-2 Nsp14 in vitro using SAM competitive inhibitors guides developing selective bisubstrate inhibitors, SLAS Discov. 26 (2021) 1200–1211, https://doi.org/10.1177/24725552211026261.
[51] T. Otava, M. Šála, F. Li, J. Fanfrlík, K. Devkota, S. Perveen, I. Chau, P. Pakarian, P. Hobza, M. Vedadi, E. Boura, R. Nencka, The structure-based design of SARS-CoV-2 nsp14 methyltransferase ligands yields nanomolar inhibitors, ACS Infect. Dis. 7 (2021) 2214–2220, https://doi.org/10.1021/acsinfecdis.1c00131.
[52] O. Bobiļeva, R. Bobrovs, I. Kaņepe, L. Patetko, G. Kalniņš, M. Šišovs, A.L. Bula, S. Gri¯nberga, M. Borodušķis, A. Ramata-Stunda, N. Rostoks, A. Jirgensons, K. Ta¯rs, K. Jaudzems, Potent SARS-CoV-2 mRNA cap methyltransferase inhibitors by bioisosteric replacement of methionine in SAM cosubstrate, ACS Med. Chem. Lett. 12 (2021) 1102–1107, https://doi.org/10.1021/acsmedchemlett.1c00140.
[53] V. Kremling, S. Falke, Y. Fernández-García, C. Ehrt, A. Kiene, B. Klopprogge, E. Scheer, F. Barthels, P. Middendorf, S. Kühn, S. Günther, M. Rarey, H. N. Chapman, D. Oberthür, J. Sprenger, SARS-CoV-2 methyltransferase nsp10-16 in complex with natural and drug-like purine analogs for guiding structure-based drug discovery, ELife 13 (2024), https://doi.org/10.7554/eLife.98310.1.
[54] S. Banerjee, S. Yadav, S. Banerjee, S.O. Fakayode, J. Parvathareddy, W. Reichard, S. Surendranathan, F. Mahmud, R. Whatcott, J. Thammathong, B. Meibohm, D. D. Miller, C.B. Jonsson, K.D. Dubey, Drug repurposing to identify nilotinib as a potential SARS-CoV-2 main protease inhibitor: insights from a computational and in vitro study, J. Chem. Inf. Model 61 (2021) 5469–5483, https://doi.org/10.1021/acs.jcim.1c00524.
[55] V. Cagno, G. Magliocco, C. Tapparel, Y. Daali, The tyrosine kinase inhibitor nilotinib inhibits SARS-CoV-2 in vitro, Basic Clin. Pharmacol. Toxicol. 128 (2021) 621–624, https://doi.org/10.1111/bcpt.13537.
[56] J. Dyall, C.M. Coleman, B.J. Hart, T. Venkataraman, M.R. Holbrook, J. Kindrachuk, R.F. Johnson, G.G. Olinger, P.B. Jahrling, M. Laidlaw, L.M. Johansen, C.M. Lear-Rooney, P.J. Glass, L.E. Hensley, M.B. Frieman, Repurposing of clinically developed drugs for treatment of middle east respiratory syndrome coronavirus infection, Antimicrob. Agents Chemother. 58 (2014) 4885–4893, https://doi.org/10.1128/AAC.03036-14.
[57] M. García, A. Cooper, W. Shi, W. Bornmann, R. Carrion, D. Kalman, G.J. Nabel, Productive replication of ebola virus is regulated by the c-Abl1 tyrosine kinase, Sci. Transl. Med. 4 (2012) 123ra24, https://doi.org/10.1126/scitranslmed.3003500.
[58] A.J. D. Francis, S. C.S, A. K.G, S. C, E.J. Variyar, Repurposing simeprevir, calpain inhibitor IV and a cathepsin F inhibitor against SARS-CoV-2 and insights into their interactions with M ^{pro}, J. Biomol. Struct. Dyn. 40 (2022) 325–336, https://doi.org/10.1080/07391102.2020.1813200.
[59] A.B. Farias, G. Candiotto, L. Siragusa, L. Goracci, G. Cruciani, E.R.A. Oliveira, B.A. C. Horta, Targeting Nsp9 as an anti-SARS-CoV-2 strategy, New J. Chem. 45 (2021) 522–525, https://doi.org/10.1039/D0NJ04909C.
[60] S.K. Behera, N. Mahapatra, C.S. Tripathy, S. Pati, Drug repurposing for identification of potential inhibitors against SARS-CoV-2 spike receptor-binding domain: an: in silico: approach, Indian J. Med. Res. 153 (2021) 132, https://doi.org/10.4103/ijmr.IJMR_1132_20.
[61] S. Ahmed, R. Mahtarin, S.S. Ahmed, S. Akter, Md.S. Islam, A.A. Mamun, R. Islam, M.N. Hossain, M.A. Ali, M.U.C. Sultana, M.D.R. Parves, M.O. Ullah, M.A. Halim, Investigating the binding affinity, interaction, and structure-activity-relationship of 76 prescription antiviral drugs targeting RdRp and Mpro of SARS-CoV-2, J. Biomol. Struct. Dyn. 39 (2021) 6290–6305, https://doi.org/10.1080/07391102.2020.1796804.
[62] H.S. Lo, K.P.Y. Hui, H.-M. Lai, X. He, K.S. Khan, S. Kaur, J. Huang, Z. Li, A.K. N. Chan, H.H.-Y. Cheung, K.-C. Ng, J.C.W. Ho, Y.W. Chen, B. Ma, P.M.-H. Cheung, D. Shin, K. Wang, M.-H. Lee, B. Selisko, C. Eydoux, J.-C. Guillemot, B. Canard, K.-P. Wu, P.-H. Liang, I. Dikic, Z. Zuo, F.K.L. Chan, D.S.C. Hui, V.C.T. Mok, K.-B. Wong, C.K.P. Mok, H. Ko, W.S. Aik, M.C.W. Chan, W.-L. Ng, Simeprevir potently suppresses SARS-CoV-2 replication and synergizes with remdesivir, ACS Cent. Sci. 7 (2021) 792–802, https://doi.org/10.1021/acscentsci.0c01186.
[63] K. Bafna, K. White, B. Harish, R. Rosales, T.A. Ramelot, T.B. Acton, E. Moreno, T. Kehrer, L. Miorin, C.A. Royer, A. García-Sastre, R.M. Krug, G.T. Montelione, Hepatitis C virus drugs that inhibit SARS-CoV-2 papain-like protease synergize with remdesivir to suppress viral replication in cell culture, Cell Rep. 35 (2021) 109133, https://doi.org/10.1016/j.celrep.2021.109133.
[64] S. Feng, X. Luan, Y. Wang, H. Wang, Z. Zhang, Y. Wang, Z. Tian, M. Liu, Y. Xiao, Y. Zhao, R. Zhou, S. Zhang, Eltrombopag is a potential target for drug intervention in SARS-CoV-2 spike protein, Infect. Genet. Evol. 85 (2020) 104419, https://doi.org/10.1016/j.meegid.2020.104419.
[65] A. Swargiary, A.K. Verma, M. Daimari, M.K. Roy, Simeprevir and eltrombopag as potential inhibitors of SARS-CoV2 proteases: a molecular docking and virtual screening approach to combat COVID-19, (n.d.).
[66] M.M. Yaşar, E. Yaşar, N. Yorulmaz, E. Tenekeci, İ.H. Sarpün, E. Eroğlu, An in silico investigation of allosteric inhibition potential of Dihydroergotamine against Sars-

CoV-2 Main Protease (MPro), Turk. Comp. Theo Chem. (TCTC) 7 (2023) 14–36, https://doi.org/10.33435/tcandtc.1121985.
[67] A.B. Gurung, M.A. Ali, J. Lee, M. Abul Farah, K.M. Al-Anazi, *In silico* screening of FDA approved drugs reveals ergotamine and dihydroergotamine as potential coronavirus main protease enzyme inhibitors, Saudi J. Biol. Sci. 27 (2020) 2674–2682, https://doi.org/10.1016/j.sjbs.2020.06.005.
[68] K.B. Ku, H.J. Shin, H.S. Kim, B.-T. Kim, S.-J. Kim, C. Kim, Repurposing screens of FDA-approved drugs identify 29 inhibitors of SARS-CoV-2, J. Microbiol. Biotechnol. 30 (2020) 1843–1853, https://doi.org/10.4014/jmb.2009.09009.
[69] S. Stagnoli, G. Macari, P. Corsi, B. Capone, A. Vidaurrazaga, J. Ereño-Orbea, A. Ardá, F. Polticelli, J. Jiménez-Barbero, N.G. Abrescia, I. Coluzza, Targeting the spike: repurposing mithramycin and dihydroergotamine to block SARS-CoV-2 infection, ACS Omega 8 (2023) 43490–43499, https://doi.org/10.1021/acsomega.3c02921.
[70] M. Sanford, Simeprevir: a review of its use in patients with chronic Hepatitis C virus infection, Drugs 75 (2015) 183–196, https://doi.org/10.1007/s40265-014-0341-2.
[71] Olysio Prices, Coupons, Copay & Patient Assistance, Drugs.Com (n.d.). http://www.drugs.com/price-guide/olysio (accessed May 16, 2024).
[72] Tasigna Prices, Coupons, Copay & Patient Assistance, Drugs.Com (n.d.). http://www.drugs.com/price-guide/tasigna (accessed May 16, 2024).
[73] S. Sirrs, H. Anderson, B. Jiwani, L.D. Lynd, E. Lun, B. Nakagawa, D. Regier, S. Rizzardo, A. McFarlane, Expensive drugs for rare diseases in Canada: what value and at what cost? Health Pap. 21 (2023) 10–26, https://doi.org/10.12927/hcpap.2023.27000.
[74] M. Zampoli, B.M. Morrow, G. Paul, Real-world disparities and ethical considerations with access to CFTR modulator drugs: mind the gap!, Front Pharm. 14 (2023) 1163391, https://doi.org/10.3389/fphar.2023.1163391.